International Journal of Recent Technology and Engineering (IJRTE)
ISSN: 2277-3878 (Online), Volume-8 Issue-4, November 2019

Reconstruction Error Analysis of Skin Lesion Images using Orthogonal Moments

Sudhakar Singh, Masood Alam, Shabana Urooj

Abstract: ***Orthogonal moments (OMs) are amongst the superlative region centered shape descriptors. These OMs retain lowest facts redundancy. Zernike Moments (ZM) and pseudo Zernike Moments (PZM) are tested with respect to rotation invariance, and scale invariance for skin lesion images. Image reconstruction is executed for various orders of two different orthogonal moments; ZM and PZM. Reconstruction errors are also computed. This paper examines the impact of these errors on the features of OMs and executes a relative study of these errors on the precise calculation of the two major OMs: ZMs and PZMs.***

Keywords: Orthogonal Moments Invariants, ZM, PZM, PSO SVM.

I. INTRODUCTION

Orthogonal Rotation-Invariant Moments (ORIMs) are very significant features for image analysis. Moments hold important data in images, and they are invariant. ORIMs contain ZM and PZM, [1],[2] Zernike moments, were planned by Zernike in 1934 as the eigenfunctions of differential equation. ZM can also be produced by Legendre Polynomials with firm constraints 1954, found by Bhatia and Wolf in 1954. Sergio Dominguez [3] proposed a technique for the recognition of 3-D object and pose analysis. Chandan et al.[4] proposed a technique for the error computation, Sheng et al. proposed OFMMs [5],[8] for pattern recognition. The amounts of OMs are invariant to the variation of the signal [6]. OMs are digitized together geometrically on the unit disk and arithmetically in the orthogonal function values for imaging applications [6],[1]. Certainly, a bundel of pixels are designated to overlap the unit disk and a value is allocated for each orthogonal function and each selected pixel [10]. Straight approaches determine the orthogonal function value for a pixel by sampling the functions at one or numerous positions of the pixel [11].

Manuscript published on November 30, 2019.
* Correspondence Author
Sudhakar Singh, Department of Biomedical Engineering, LPU, Phagwara, Punjab, India
Masood Alam, Department of Mathematics and IT, Centre for Prepatory Studies, Sultan Qaboos University,
Muscat, Sultanate of Oman
Shabana Urooj, Department of Electrical Engineering, Gautam Buddha University, Greater Noida, U.P., India

In image investigation, pattern recognition [12], texture arrangement [13], image indexing and target direction assessment OM played very important role. Orthogonal moments [13]–[16] are noise resistant [6] and are used as a base to create moments with new belongings. Few additional efforts had been made to decline calculation time of the orthogonal moments [17]. However, digitization negotiations the precision of the orthogonal moments.

Two types of errors had been identified direct method in digitization .The first error derives from the approximation of the continuous unit disk by a finite set of pixels, called geometric error.

The second error is after sampling orthogonal functions. Liao and Pawlak proposed a method for selecting the radius of the disk and thus the number of pixels to control the geometric error, numerical error when determining the orthogonal function values [21]. Recently, Xin et al. developed a technique to compute Zernike moments in polar space [11]. The Zernike orthogonal moments, being invariant to rotations and reflections, have been suggested to be an attractive alternative. This set of orthogonal functions has been introduced by Zernike as a basic tool for representation of a wave front function for optical systems with circular pupils. Since then the radial polynomials have been found important in applications ranging from pattern recognition, shape analysis, optical engineering, and medical imaging to eye diagnostic [18].

II. PROPOSED METHODOLOGY

A. Orthogonal Rotation Invariant Moment (ORIM)

The proposed method has been applied to capture the pattern and edge qualities of the image. It is well defined that Zernike polynomials are orthogonal to each other, these moments can characterize the qualities of an image with no idleness or coincide of facts between the moments. Because of these unique properties, these features have broadly been used in different types of applications [9][18]. It has been used in pattern-based image recovery in edge detection and like a feature set in model recognition.

The Zernike polynomials are orthogonal. Therefore it can draw out the Zernike moments from a ROI irrespective of the shape of the target [4]. The formulation of Zernike moment appears to be very favored, outperforming the options (in phrase of noise resilience, information redundancy and reconstruction capability).

Image function f (j,k) is defined in four-sided engagements of pixels with j represents rows and k represents column.

If the four-sided image considered through N rows and N columns. For the computation of OMs, a transformation is done that translates the square domain of N × N pixels hooked on a unit disk. The subsequent mapping is the furthermost method to comprehend the objective.

$$x_j = \frac{2j+1-N}{D}$$
$$y_k = \frac{2k+1-N}{D} \qquad (1)$$

Where j,k= 0,12,….N-1

With

$$D=\begin{cases} N\sqrt{2} & \text{for outer disk} \\ N & \text{for inner disk} \end{cases}$$

The mapping is shown in Fig.1, where Fig.1 (a) is an 8×8 pixel grid, obeying the condition is as shown in Fig.1 (b). The external unit disk encircling the whole image is exposed in Fig.1(c).

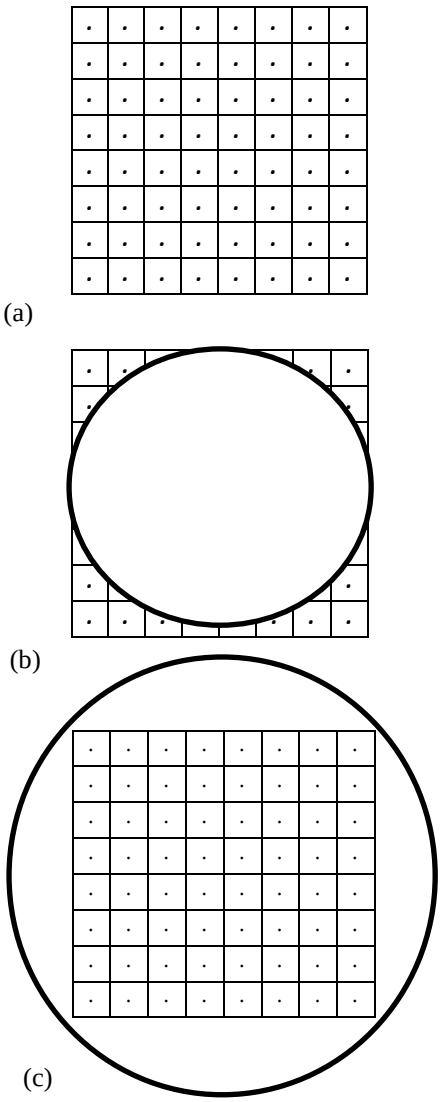

Figure 1 (a) An 8×8 pixel grid, (b) inside circular disk approximated by square grids, and (c) outer circular disk containing complete square image grid

Consequently, the OMs are well-defined for image function f (xj, yk) as follows in equation (2).

$$A_{m,n} = \frac{m+1}{\pi}\sum_{j=o}^{N-1}\sum_{k=0}^{N-1} f(x_j,y_k)V^*_{m,n}(x_j,y_k)\Delta^2 \qquad (2)$$

Here $\frac{m+1}{\pi}$ is normalizing factor, m is non-negative integer called order, and n is integer called repetition and $V^*_{m,n}(x,y)$ is complex conjugate of $V_{m,n}(x,y)$ moment basis function $V_{m,n}(x,y)$ can be defined as below.

$$V_{m,n}(x,y) = R_{m,n}(\rho)e^{jn\theta} \qquad (3)$$

where zand $j=\sqrt{-1}$, $R_{m,n}(\rho)$ is radial polynomial. The image function f(x, y) can be characterized as

$$e = \frac{\sum_{j=0}^{N-1}\sum_{k=0}^{N-1}(f(x_j,y_k)-f_1(x_j,y_k))^2}{\sum_{j=0}^{N-1}\sum_{k=0}^{N-1}f^2(x_j,y_k)} \qquad (4)$$

Modified radial polynomial can be expressed as

$$A_{m,n} = \frac{m+1}{\pi}\sum_{j=o}^{N-1}\sum_{k=0}^{N-1} f(x_j,y_k)V^*_{m,n}(x_j,y_k)\Delta^2 \qquad (5)$$

Here $\Delta = \frac{2}{D}$, The discrete recreated image $f_1(x, y)$ and the comparative reconstruction error e is given by Eqs. (6) and (7), correspondingly.

$$f_1(j,k) = \sum_m\sum_n A_{m,n}V_{m,n}(x_j,y_k) \qquad (6)$$

where j,k=0,1,2……..N-1

$$e = \frac{\sum_{j=0}^{N-1}\sum_{k=0}^{N-1}(f(x_j,y_k)-f_1(x_j,y_k))^2}{\sum_{j=0}^{N-1}\sum_{k=0}^{N-1}f^2(x_j,y_k)} \qquad (7)$$

A. Zernike Polynomial

Zernike Polynomial for an image using current pixel f(x,y) is explained as

$$R^Z{}_{m,n}(\rho) = \sum_{s=0}^{(m-|n|)/2}\frac{(-1)^s(m-s)!\rho^{m-2s}}{s!\left(\frac{m+|n|}{2}-s\right)!\left(\frac{m-|n|}{2}-s\right)!} \qquad (8)$$

where $|n| \le m$ and $m-|n|$ =even

B. Pseudo Zernike Polynomial

Pseudo Zernike Polynomial for an image using current pixel f(x,y) is explained as below

$$R^P{}_{m,n}(\rho) = \sum_{s=0}^{(m-|n|)}\frac{(-1)^s(2m+1-s)!\rho^{m-s}}{s!(m+|n|+1-s)!(m-|n|-s)!} \qquad (9)$$

Where $m \le n$

III. RESULTS AND DISCUSSION

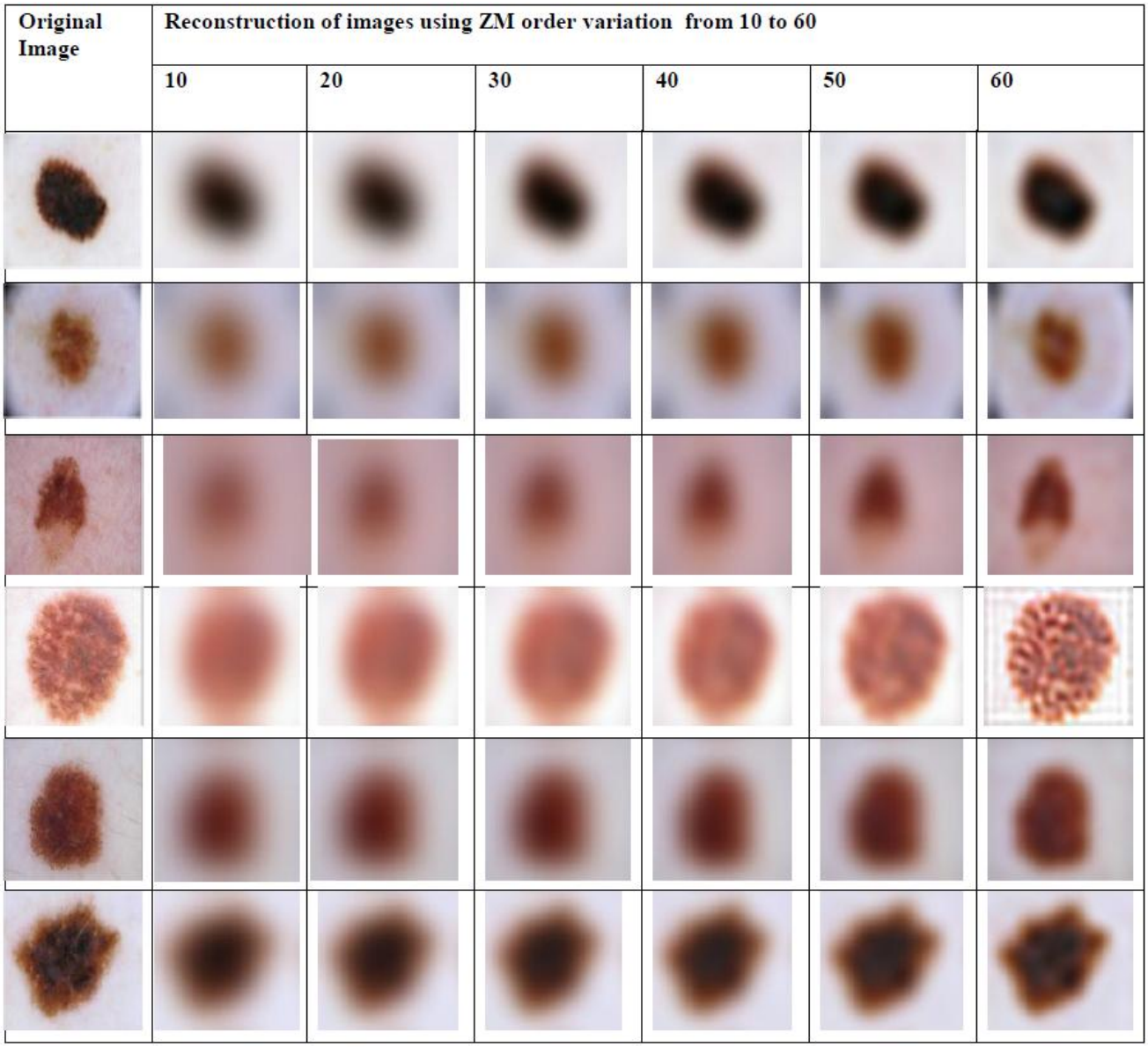

Figure 2: Reconstructed image of 256 ×256 pixels using ZM at various orders

Table 1: Reconstruction Error of six different Images using ZM

Image No.	Reconstruction Error of ZM by varying the order from 10 to 60							
	10	20	30	40	50	60	70	80
1.	0.0424	0.0343	0.0052	0.0032	0.0014	0.0011	0.0011	0.0011
2.	0.0521	0.0362	0.0060	0.0041	0.0017	0.0016	0.0016	0.0016
3.	0.0328	0.0281	0.0041	0.0036	0.1200	0.0011	0.0011	0.0011
4.	0.2300	0.0437	0.0097	0.0067	0.0021	0.0018	0.0018	0.0017
5.	0.0432	0.0298	0.0078	0.0063	0.0190	0.0010	0.0009	0.0010
6.	0.0401	0.0276	0.0063	0.0060	0.0020	0.0012	0.0012	0.0012

Original Image	Reconstruction of images using PZM order variation from 10 to 60					
	10	20	30	40	50	60
	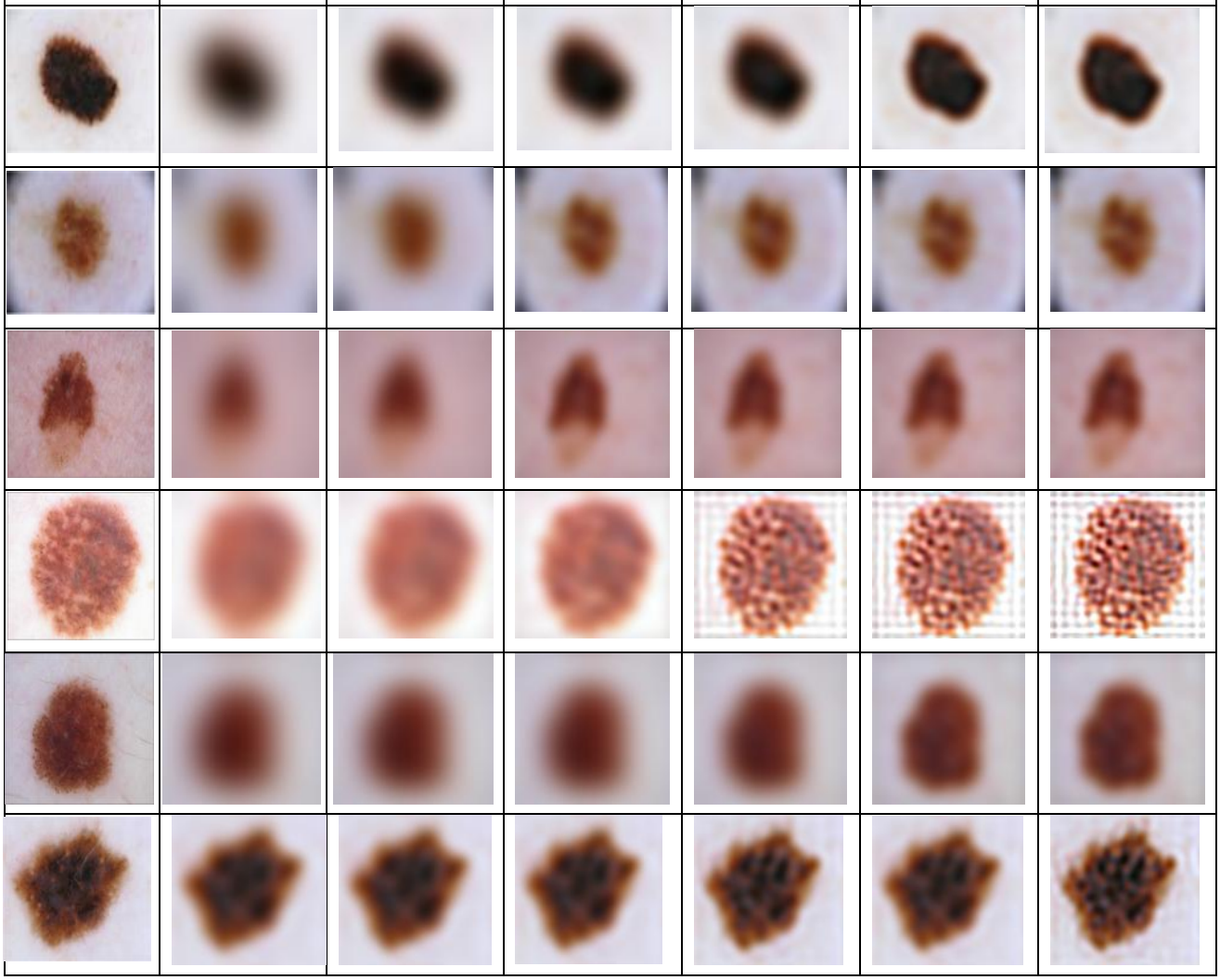					

Figure 3: Reconstructed image of 256 ×256 pixels using PZM at various orders

Table 2: Reconstruction Error of six different Images using PZM

Image No.	Reconstruction Error of PZM by varying the order 10 to 60							
	10	20	30	40	50	60	70	80
1.	0.0321	0.0201	0.0042	0.0030	0.0012	0.0008	0.0008	0.0008
2.	0.0410	0.0241	0.0056	0.0038	0.0014	0.0012	0.0013	0.0012
3.	0.0286	0.0263	0.0032	0.0032	0.0014	0.0009	0.0009	0.0009
4.	0.0401	0.0387	0.0082	0.0054	0.0019	0.0011	0.0011	0.0011
5.	0.0321	0.0251	0.0062	0.0041	0.0018	0.0010	0.0009	0.0010
6.	0.0361	0.0231	0.0054	0.0041	0.0016	0.0011	0.0011	0.0011

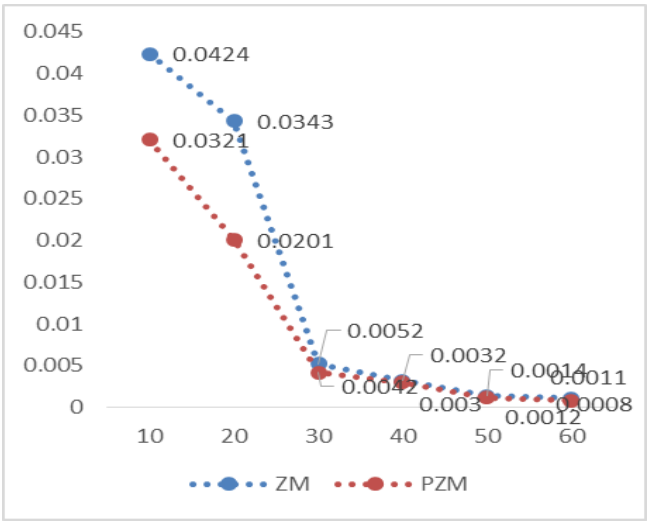

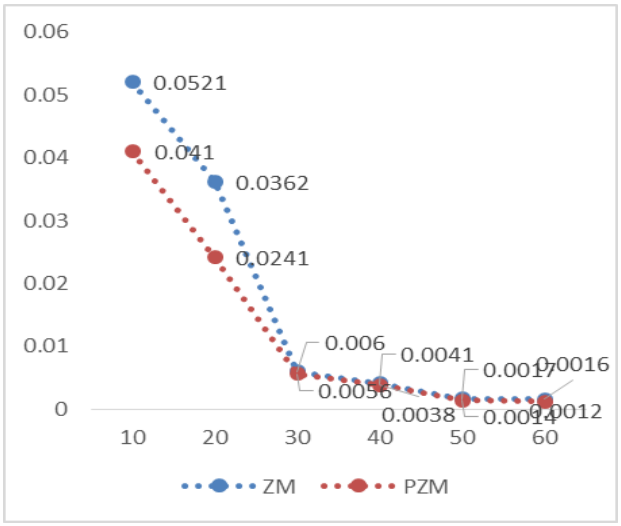

Figure 4(a) Rconstruction ErrorVS Order plot of ZM & PZM for image 1, 4(b) Rconstruction ErrorVS Order plot of ZM & PZM for image 2

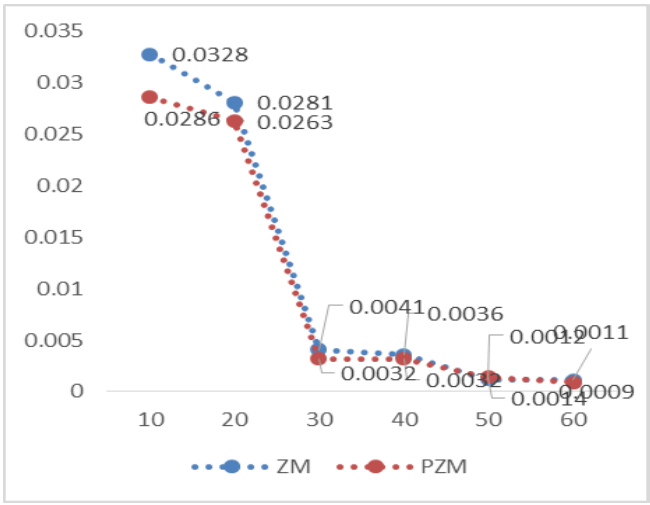

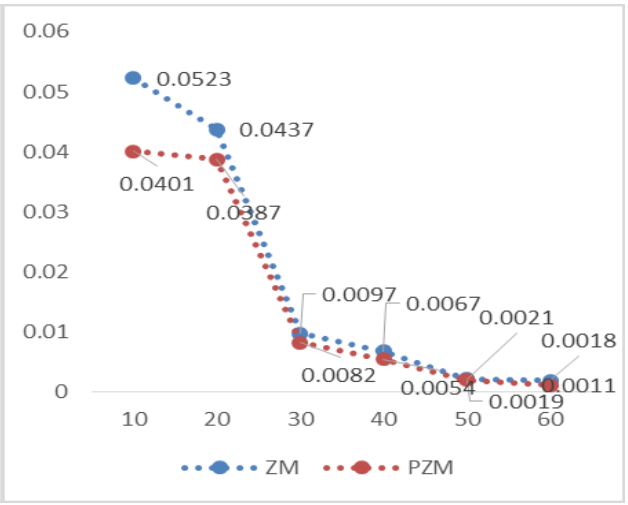

Figure 4(c) Reconstruction Errors VS Order plot of ZM & PZM for image 3, 4(d) Reconstruction Errors Order plot of ZM & PZM for image 4

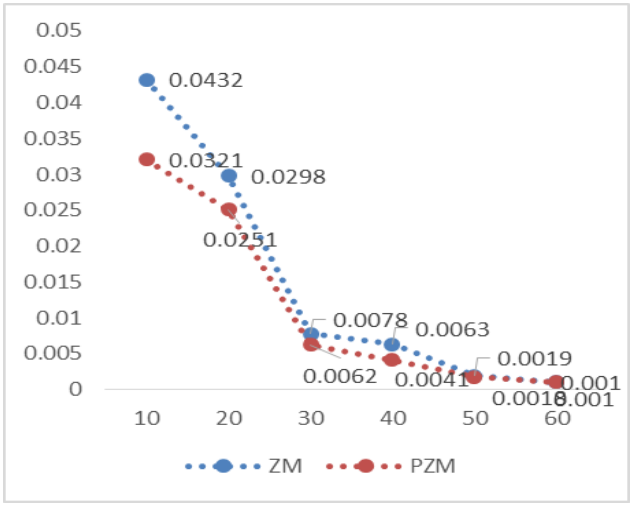

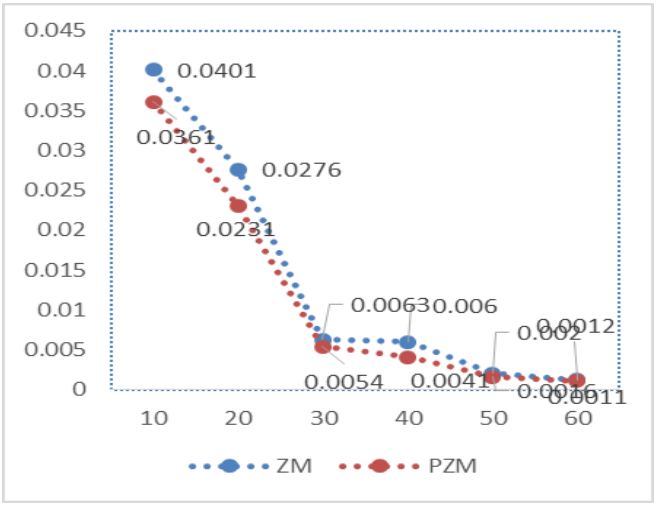

Figure 4(e) Reconstruction Error vs Order plot of ZM & PZM for image 5, 4(f) Reconstruction Error vs Order plot of ZM & PZM for image 6

Figure 2,3 shows the reconstructed images using ZM and PZM respectively. Table 1,2 shows the reconstruction error achieved by ZM and PZM respectively. Figure4 (a) presents the reconstruction error by ZM and PZM for the image, the error is minimum at moment's order 60 and maximum at moment order10. If moment order further increases beyond the 60 to 90 the reconstruction error remains same as shown in table 1,2. Figure4(b) shows the reconstruction error plot for the test image 2, the error is minimum at moment order 60 and maximum at moment order 10 for both ZM and PZM. Figure4(c) shows the reconstruction error computed by ZM and PZM for the test images 3. The error is minimum for the moment order 60 and maximum for the moment order 10. Figure4 (d) presents the calculated reconstruction error for the test image 4 by using ZM and PZM. The achieved error is maximum at moment order 10 and minimum at momenta order 60. Figure4 (e) shows the reconstruct in error plot for the ZM and PZM of test image 5. The achieved error is minimum at moment order 60 and maximum at moment order 10. Figure4 (f) presents the plot of reconstruction error and moment order for the test image 6. The obtained error is minimum for the moment order 60 and maximum for the moment order 10.

IV. CONCLUSION

In this chapter orthogonal moments have been proposed for analysis of melanoma images. Moment invariants available in literature and past research have not made any significant contribution in melanoma image analysis. Obtained results from image reconstruction using PZM gives better accuracy as compare to ZM as shown in figure 4(a) to 4(f). ORIM are very sensitive to noise and no redundant hence very limited moments are required for the classification as compare to the color features and hence may provide efficient analysis of images. It is significant to classify the disease assessment in a better way by analyzing the image. Computer analysis available so far still need much specialized environment and tools especially for the less skilled skin experts. The proposed melanoma classification algorithm may be utilized for betterment to improve diagnostic accuracy of melanoma and hence the societal welfare.

REFERENCES

1. S. Urooj, S. P. Singh, and A. Q. Ansari, Computer Aided Detection of Breast Cancer using Pseudo Zernike Moment as a Texture Descriptors, vol. 651, no. March. 2013.
2. S. P. Singh and S. Urooj, "Accurate and Fast Computation of Exponent Fourier Moment," Arab. J. Sci. Eng., vol. 42, no. 8, pp. 3299–3306, 2017.
3. S. Dominguez, "Simultaneous recognition and relative pose estimation of 3D objects using 4D orthonormal moments," Sensors (Switzerland), vol. 17, no. 9, 2017.
4. C. Singh and R. Upneja, "Error analysis in the computation of orthogonal rotation invariant moments," J. Math. Imaging Vis., vol. 49, no. 1, pp. 251–271, 2014.
5. C. Kan and M. D. Srinath, "Invariant character recognition with Zernike and orthogonal Fourier-Mellin moments," Pattern Recognit., vol. 35, no. 1, pp. 143–154, 2002.
6. H. Zhang, Z. Li, and Y. Liu, "Fractional orthogonal fourier-mellin moments for pattern recognition," in Communications in Computer and Information Science, 2016, vol. 662, pp. 766–778.
7. H. Zhang, H. Z. Shu, P. Haigron, B. S. Li, and L. M. Luo, "Construction of a complete set of orthogonal Fourier-Mellin moment invariants for pattern recognition applications," Image Vis. Comput., vol. 28, no. 1, pp. 38–44, 2010.
8. Y. Sheng and H. H. Arsenault, "Experiments on pattern recognition using invariant Fourier–Mellin descriptors," J. Opt. Soc. Am. A, vol. 3, no. 6, p. 771, 1986.
9. A. Khotanzad and Y. H. Hong, "Invariant Image Recognition by Zernike Moments," IEEE Trans. Pattern Anal. Mach. Intell., vol. 12, no. 5, pp. 489–497, 1990.
10. T. V. Hoang and S. Tabbone, "Erratum: Generic orthogonal moments: Jacobi-Fourier moments for invariant image description (Pattern Recognition)," Pattern Recognition, vol. 46, no. 11. pp. 3148–3155, 2013.
11. X. Li and A. Song, "A new edge detection method using Gaussian-Zemike moment operator," CAR 2010 - 2010 2nd International Asia Conference on Informatics in Control, Automation and Robotics, vol. 1. pp. 276–279, 2010.
12. Z. Ping, H. Ren, J. Zou, Y. Sheng, and W. Bo, "Generic orthogonal moments: Jacobi-Fourier moments for invariant image description," Pattern Recognit., vol. 40, no. 4, pp. 1245–1254, 2007.
13. R. Dhir, "Moment based invariant feature extraction techniques for Bilingual Character Recognition," ICETC 2010 - 2010 2nd Int. Conf. Educ. Technol. Comput., vol. 4, 2010.
14. Z. Shao, H. Shu, J. Wu, B. Chen, and J. L. Coatrieux, "Quaternion Bessel-Fourier moments and their invariant descriptors for object reconstruction and recognition," Pattern Recognit., vol. 47, no. 2, pp. 603–611, 2014.
15. J. Mennesson, C. Saint-Jean, and L. Mascarilla, "Color Fourier-Mellin descriptors for image recognition," Pattern Recognit. Lett., vol. 40, no. 1, pp. 27–35, 2014.
16. S. Jain, V. Jagtap, and N. Pise, "Computer aided melanoma skin cancer detection using image processing," in Procedia Computer Science, 2015, vol. 48, no. C, pp. 736–741.
17. Y. Sheng and L. Shen, "Orthogonal Fourier–Mellin moments for invariant pattern recognition," J. Opt. Soc. Am. A, vol. 11, no. 6, p. 1748, 1994.
18. B. H. Shekar and D. S. Rajesh, "Affine Normalized Krawtchouk Moments Based Face Recognition," in Procedia Computer Science, 2015, vol. 58, pp. 66–75.
19. Sudhakar Singh and Shabana Urooj. Analysis of Chronic Skin Diseases using Artificial Neural Network. International Journal of Computer Applications 179(31):7-13, April 2018.
20. M. Sheha, M. Mabrouk, and A. Sharawy, "Automatic detection of melanoma skin cancer using texture analysis," Int. J. Comput. …, vol. 42, no. 20, pp. 22–26, 2012.
21. S. M. Pereira, M. A. C. Frade, R. M. Rangayyan, and P. M. Azevedo-Marques, "Classification of color images of dermatological ulcers," IEEE J. Biomed. Heal. Informatics, vol. 17, no. 1, pp. 136–142, 2013.